

A Convolution-Based Gait Asymmetry Metric for Inter-Limb Synergistic Coordination

Go Fukino

Kanta Tachibana

Abstract—This study focuses on the velocity patterns of various body parts during walking and proposes a method for evaluating gait symmetry. Traditional motion analysis studies have assessed gait symmetry based on differences in electromyographic (EMG) signals or acceleration between the left and right sides. In contrast, this paper models intersegmental coordination using an LTI system and proposes a dissimilarity metric to evaluate symmetry. The method was tested on five subjects with both symmetric and asymmetric gait.

Index Terms—Gait analysis, convolution, transfer function, time-series, symmetry, OpenPose.

I. INTRODUCTION

Since the advent of *Homo sapiens*, bipedal locomotion has been a fundamental human movement, characterized by alternating cyclic motion. This study focuses on the velocity patterns of various body parts during walking and explores a method for evaluating gait symmetry. Previous studies evaluating gait symmetry have primarily relied on metrics such as maximum, minimum, and mean values or have visually assessed time-series patterns through graphical representations. For instance, Wang et al. [1] and Li et al. [2] assessed asymmetry in knee flexion and extension during post-stroke gait using motion data and electromyography (EMG), focusing on the maximum and minimum knee joint angles and lower limb EMG signals. Rathore et al. [3] investigated asymmetrical gait in unilateral amputees using prosthetic limbs by employing a knee flexion angle potentiometer and a foot pressure sensor to analyze peak knee flexion angles and ground reaction forces. D’Arco et al. [4] evaluated gait symmetry based on plantar pressure parameters obtained from smart insoles. Similarly, Loiret et al. [5] utilized foot pressure sensors, as in Rathore et al. [3], but specifically examined the peak values of ground reaction forces at the thigh and hip level to assess symmetry. Williamson et al. [6] used accelerometers to evaluate symmetry based on the mean acceleration values. While these studies [1–5] incorporate temporal parameters such as stance duration and gait cycle time, they primarily focus on maximum, minimum, and average values of physical quantities. However, they do not perform detailed analyses of time-series patterns. The studies conducted by Qin et al. and Yan et al. [7]–[10] analyzed gait symmetry by plotting simultaneously measured left and right electrostatic potential samples—generated through friction between the body, the floor, or clothing—on a plane and applying principal component analysis (PCA). However, these studies [7]–[10] do not take into account the sequential nature of the time-series data (i.e., that sample n is followed

by sample $n + 1$) or the nonlinear characteristics of time-series patterns. Several studies have investigated gait symmetry through detailed analysis of time-series patterns. Yoge et al. [11] evaluated gait symmetry in patients with Parkinson’s disease and elderly individuals at risk of falling using a foot pressure sensor system, considering swing time (the duration a foot remains off the ground during walking). Adamczyk et al. [12] estimated velocity from ground reaction forces and assessed gait symmetry through autocorrelation. Anna et al. [13] and Zhang et al. [14] employed wearable accelerometers to measure acceleration in both thighs and lower legs, using cross-correlation to evaluate symmetry. Gouwanda et al. [15] and Sheng et al. [16] proposed a symmetry evaluation method based on cross-correlation of angular velocity data obtained from wireless gyroscopes. Khoo et al. [17] assessed gait symmetry using time-series data of knee joint angles and joint moments. Arauz et al. [18] utilized motion capture technology to analyze changes in joint angles during treadmill walking (both normal-speed and high-speed conditions) to evaluate gait symmetry. Lena et al. [19] proposed a symmetry index by integrating a symmetry function derived from time-series data of foot joint angles over the gait cycle. Additionally, Diaz et al. [20] analyzed the vertical trajectory of the body’s center of mass in lower-limb amputees (particularly transfemoral amputees) and introduced a frequency-domain gait symmetry evaluation method using Discrete Fourier Transform (DFT). These studies have compared left and right time-series patterns in both the time and frequency domains as symmetry evaluation metrics, employing analytical approaches similar to Proposed Method I in this study. None of the existing methods evaluate the left-right difference in Time Series Pairs (TSPs), as proposed in Proposed Method II of this study. Additionally, these conventional studies rely on specialized equipment, making them less accessible for general use. This study aims to develop a simple and practical gait symmetry evaluation system that does not require dedicated devices, utilizing smartphone video recordings and OpenPose. OpenPose extracts skeletal information from video footage captured by a standard camera. Since no specialized equipment is needed, this approach significantly reduces the burden of both preparation and measurement, making gait symmetry analysis more accessible and convenient. The objective of this study is to propose a dissimilarity metric for evaluating the left-side and right-side intersegmental coordination systems underlying Time Series Pairs (TSPs) extracted from video recordings of gait, without the need for specialized equipment. Furthermore,

this study aims to determine whether the proposed metric can effectively quantify left-right asymmetry in gait patterns.

II. THEORETICAL BACKGROUND

In this study, we propose two indices of left-right symmetry for analyzing cyclic alternating movements such as walking. Proposed Method I: A method that compares left and right movement patterns by shifting half a walking cycle; Proposed Method II: A method that compares coordinated systems based on transfer functions. Proposed Method I measures waveform similarity by shifting the movement velocity calculated from the left and right body coordinates by $+1/4$ cycle for the left side and $-1/4$ cycle for the right side. Proposed Method II uses the transfer function between time-series signals of two body parts. Specifically, it evaluates left-right symmetry using a non-similarity index based on an LTI (Linear Time Invariant) system, where the movement of the wrist (horizontal or vertical) is analyzed in relation to the movement of the ankle (horizontal or vertical).

A. 1/4 Cycle Shift Transformation

For a discrete-time series of period N , denoted as

$$x(n), \quad n = 0, 1, \dots, N-1,$$

the Fourier coefficient $X(k) \in \mathbb{C}$ of waveform k is given by:

$$X(k) = \sum_{n=0}^{N-1} x(n) \exp\left(-j \frac{2\pi kn}{N}\right), \quad k = -K, \dots, -1, 0, 1, \dots, K$$

where j is the imaginary unit and $K = \lfloor \frac{N}{2} \rfloor$.

For a periodic function $x(t)$ with period T , the $\frac{1}{4}$ cycle shift transformation is represented as:

$$x\left(t - \frac{T}{4}\right) = \sum_{k=-\infty}^{\infty} X(k) \exp\left(j \frac{2\pi k}{T} \left(t - \frac{T}{4}\right)\right).$$

This becomes:

$$\begin{aligned} &= \sum_{k=-\infty}^{\infty} X(k) \exp\left(j \frac{2\pi kt}{T}\right) \exp\left(-j \frac{\pi k}{2}\right), \\ &= \sum_{k=-\infty}^{\infty} (-j)^k X(k) \exp\left(j \frac{2\pi kt}{T}\right). \end{aligned}$$

This means that multiplying each Fourier coefficient $X(k)$ by $-j$ results in a $+\frac{1}{4}$ cycle shift, while multiplying by j results in a $-\frac{1}{4}$ cycle shift.

For observed discrete-time right-side and left-side data $x(n)$ and $y(n)$, respectively, with sample size M (including 3–6 strides), this transformation shifts the left side by $+\frac{1}{4}$ cycle and the right side by $-\frac{1}{4}$ cycle, resulting in a total shift of $\frac{1}{2}$ cycle.

SYMMETRY EVALUATION

The left-right movement symmetry is then evaluated using the correlation coefficient:

$$\rho = \frac{\text{cov}(x, y)}{\sigma_x \sigma_y},$$

where:

$$\begin{aligned} \bar{x} &= \frac{1}{M} \sum_{n=0}^{M-1} x[n], \quad \bar{y} = \frac{1}{M} \sum_{n=0}^{M-1} y[n], \\ \sigma_x &= \sqrt{\frac{1}{M} \sum_{n=0}^{M-1} (x[n] - \bar{x})^2}, \quad \sigma_y = \sqrt{\frac{1}{M} \sum_{n=0}^{M-1} (y[n] - \bar{y})^2}. \end{aligned}$$

B. Transfer Function-Based Symmetry

Let the relationship between input and output Let the relationship between input and output discrete-time signals $x[n]$ and $y[n]$, for $n = 0, \dots, N-1$, be modeled as a Linear Time-Invariant (LTI) system. The sequences are transformed using the Z-transform:

$$\begin{aligned} X(z) &= x[0]z^0 + x[1]z^{-1} + \dots + x[N-1]z^{-N+1}, \\ Y(z) &= y[0]z^0 + y[1]z^{-1} + \dots + y[N-1]z^{-N+1}. \end{aligned}$$

The system's transfer function is defined as:

$$G(z) = \frac{Y(z)}{X(z)}.$$

To evaluate movement symmetry, two symmetrical pairs of body parts are selected. Let $G_1(z) = \frac{B(z)}{A(z)}$ be the transfer function for the right-side system, and $G_2(z) = \frac{Y(z)}{X(z)}$ for the left-side system. The movement is considered symmetric if the transfer functions are approximately equal:

$$A(z)Y(z) \approx X(z)B(z).$$

Assume: - $a[n]$: horizontal/vertical speed of the right ankle, - $b[n]$: speed of the right wrist, - $x[n]$: speed of the left ankle, - $y[n]$: speed of the left wrist.

Then the Z-domain products are:

$$\begin{aligned} A(z)Y(z) &= \left(\sum_{n=0}^{N-1} a[n]z^{-n} \right) \left(\sum_{n=0}^{N-1} y[n]z^{-n} \right) = \sum_{k=0}^{2N-2} (a * y)[k]z^{-k}, \\ X(z)B(z) &= \left(\sum_{n=0}^{N-1} x[n]z^{-n} \right) \left(\sum_{n=0}^{N-1} b[n]z^{-n} \right) = \sum_{k=0}^{2N-2} (x * b)[k]z^{-k}, \end{aligned}$$

where $*$ denotes linear convolution, and:

$$(a * y)[k] = \sum_{l=0}^k a[l]y[k-l], \quad (x * b)[k] = \sum_{l=0}^k x[l]b[k-l],$$

assuming $a[n] = b[n] = x[n] = y[n] = 0$ for all $n \notin [0, N]$.

Let:

$$\mathbf{u} = a * y, \quad \mathbf{v} = x * b,$$

where $\mathbf{u}, \mathbf{v} \in \mathbb{R}^{2N-1}$.

DISSIMILARITY MEASURE FOR SYMMETRY

To quantify the symmetry of movement, the dissimilarity between the two LTI systems is defined as:

$$\text{Dis}((a, b), (x, y)) = \frac{\|\mathbf{u} - \mathbf{v}\|^2}{\|\mathbf{u}\| \cdot \|\mathbf{v}\|},$$

where $\|\cdot\|$ denotes the Euclidean norm. A smaller dissimilarity implies more symmetric movement between the left and right side systems.

This measure is used to evaluate movement symmetry. Fig. 1 illustrates an example of dissimilarity evaluation between LTI systems.

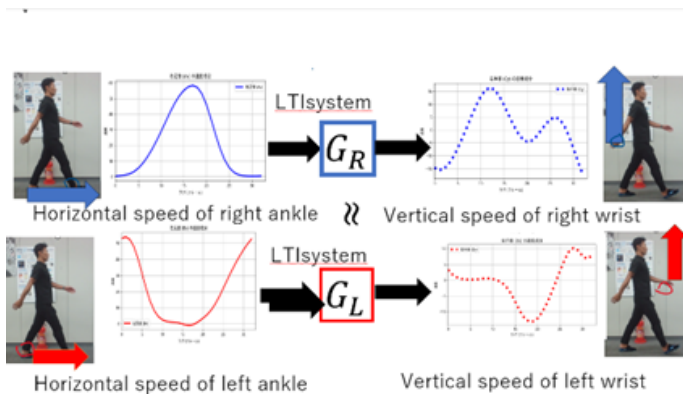


Fig. 1. Illustration of dissimilarity metric between LTI systems

III. METHODOLOGY AND EXPERIMENTS

We recorded the normal walking motion (referred to as Motion S) of five healthy male subjects. Immediately after, we asked them to perform an extremely asymmetrical walking motion (referred to as Motion A) and recorded it as well. Both motions were filmed from a lateral view at a distance of approximately 2 meters using a camera. The camera used was an LED light web camera (model NB 05) with a frame rate of 30 fps. OpenPose was used to extract joint coordinates for both Motion S and Motion A. The tracked joints included both ankles, both knees, both hips, both wrists, and both shoulders. Simultaneously, the confidence score for each joint coordinate estimation was recorded for each frame. If a joint was occluded or difficult to estimate, its confidence score dropped below 0.5, and its coordinates were not recorded. In cases where the confidence score was 0.5 or lower, linear interpolation was applied using the coordinates from adjacent frames. Next, a moving average filter with a window size of 3 was applied to smooth the data. Figure 2 illustrates a single frame of normal walking, while Figure 3 shows a single frame of asymmetric walking. Table 1 summarizes the stride count, the number of frames in which the entire body of the subject is visible, and the gait cycle (in frames) computed via autocorrelation analysis for both symmetric and asymmetric walking motions for each subject.

TABLE I
RECODED NUMBER OF STRIDES, FRAMES AND WALKING CYCLE IN SYMMETRIC AND ASYMMETRIC GAIT MOTION

symmetri Gait Motion			
subject	motion S		
	stride	frames	cycle
1	3	80	33
2	3	75	27
3	3	60	35
4	3	100	45
5	4	100	33

Asymmetric Walk			
subject	motion S		
	stride	frames	cycle
1	7	150	34
2	3	75	35
3	4	160	41
4	6	150	66
5	4	105	31

A. Left-Right Symmetry Index Based on 1/4 Shift Transformation

The movement velocity of each joint within a frame is calculated using the following formula:

$$v = \Delta x + \Delta y \quad (1)$$

where Δx and Δy represent the differences in horizontal and vertical coordinates between consecutive frames, respectively. The velocity is expressed in units of [Pixels/Frame].

For the left and right ankle speed time series, autocorrelation analysis is performed to determine the gait cycle. Then, a $\frac{1}{4}$ shift transformation is applied: shifting the left ankle speed by $+\frac{1}{4}$ cycle and the right ankle speed by $-\frac{1}{4}$ cycle. This transformation is used to evaluate the left-right symmetry of ankle movement.



Fig. 2. Illustration of dissimilarity metric between LTI systems

B. Symmetry Index Based on Transfer Function

In the approach using transfer functions, the left-right symmetry of movement data is evaluated based on the horizontal or



Fig. 3. Illustration of dissimilarity metric between LTI systems

vertical motion of the ankles and wrists. This method assesses whether the movements exhibit symmetry between the left and right sides. Figure 4 summarizes the horizontal and vertical velocity components used to evaluate the symmetry between the ankles and wrists.

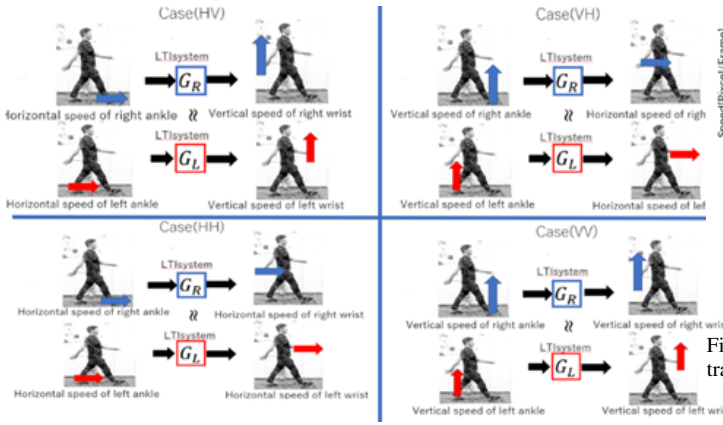


Fig. 4. Illustration of symmetry evaluation using

horizontal and vertical ankle and wrist velocity components analyzed with LTI systems. Case (HV): The horizontal speed of the ankle is used as input, and the vertical speed of the wrist is output; Case (VH): The vertical speed of the ankle is used as input, and the horizontal speed of the wrist is output; Case (HH): The horizontal speed of the ankle is used as input, and the horizontal speed of the wrist is output; Case (VV): The vertical speed of the ankle is used as input, and the vertical speed of the wrist is output.

IV. RESULTS

A. Symmetry Index Based on 1/4 Cycle Shift Transformation

Fig. 5 shows the speed of the left and right ankles for the symmetric motion S, shifted by a total of half a cycle using a 1/4 cycle shift transformation. Similarly, Fig. 6 illustrates the speed of the left and right ankles for the asymmetric motion

A, also shifted by half a cycle. Table 2 presents the correlation results of the 1/4 cycle shift transformation for five individuals.

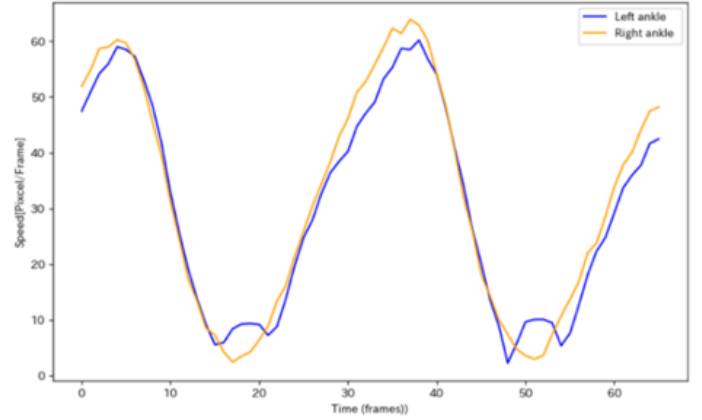


Fig. 5. Left and right ankle speed in motion S after 1/4 period shift transformation

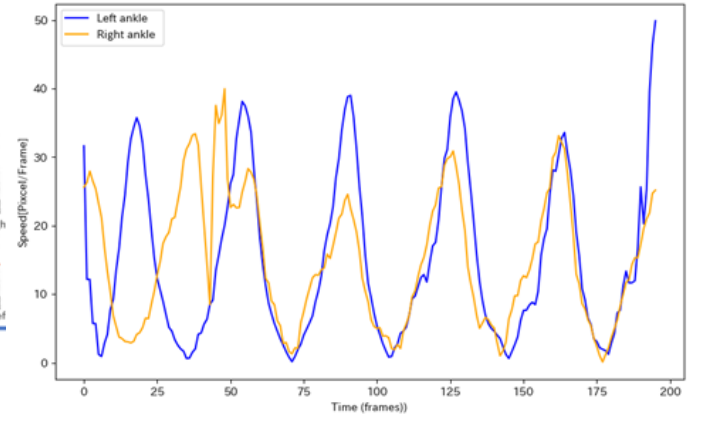


Fig. 6. Left and right ankle speed in motion A after 1/4 period shift transformation

TABLE II
CORRELATION COEFFICIENTS BETWEEN LEFT AND RIGHT ANKLE SPEED
AFTER 1/4 PERIOD SHIFT TRANSFORMATION

subject	Symmetric motion S	Asymmetric motion A
1	0.98	0.46
2	0.98	0.42
3	0.92	0.70
4	0.95	0.80
5	0.98	0.64

B. SYMMETRY INDEX BASED ON TRANSFER FUNCTION

Table 3 presents the asymmetry evaluation results for five pedestrians. The (S) column represents the dissimilarity for the symmetric motion S, while the (A) column represents the dissimilarity for motion A. For motion S, the dissimilarity was less than 1 for all five individuals across all four cases, indicating a high level of symmetry. In contrast, for motion A, the dissimilarity values were 1 or greater in cases (HV), (VH), and (VV) for all five individuals, indicating low symmetry.

However, in case (HH), the dissimilarity remained below 1 for all five individuals. Fig. 7 illustrates the horizontal and vertical speed of subject 1 during the symmetric motion S. The gait cycle was determined through autocorrelation analysis, and the data were segmented and overlaid based on the gait cycle. The horizontal axis represents frames, while the vertical axis

represents horizontal speed components. The different colors indicate:

- **Blue:** Right ankle
- **Red:** Right wrist
- **Green:** Left ankle
- **Yellow:** Left wrist

Similarly, Fig. 8 shows the horizontal and vertical speed of subject 1 during the asymmetric motion A. Fig. 9 presents the convolution diagram for case (HH) of the symmetric motion S, while Fig. 10 shows the convolution diagram for case (HH) of the asymmetric motion A.

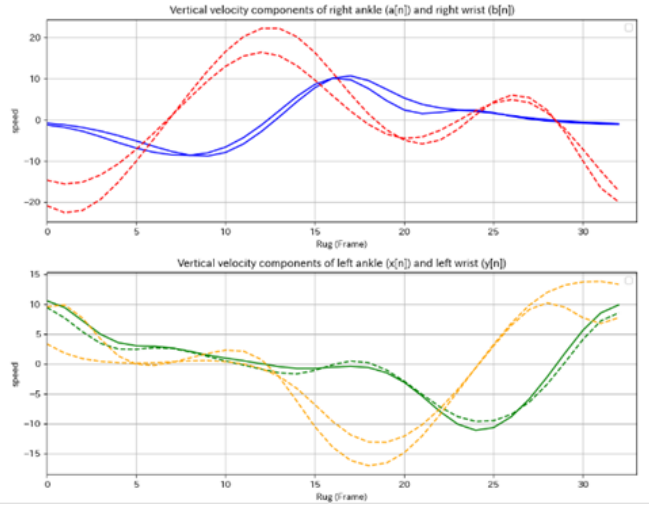


Fig. 8. Vertical speed in motion S of subject 1. Blue: Right Ankle; Red: Right Wrist; Green: Left Ankle; Yellow: Left Wrist

TABLE III
SUMMARY OF DISSIMILARITY VALUE
Dis((RIGHT ANKLE, RIGHT WRIST), (LEFT ANKLE, LEFT WRIST))

subject	case(HV)		case(VH)		case(HH)		case(VV)	
	(S)	(A)	(S)	(A)	(S)	(A)	(S)	(A)
1	0.32	1.88	0.49	1.40	0.20	0.22	0.31	1.81
2	0.62	2.97	0.39	1.60	0.29	0.43	0.92	4.40
3	0.41	2.00	0.17	0.78	0.15	0.79	0.18	0.80
4	0.64	2.00	0.57	1.94	0.44	0.52	0.80	2.13
5	0.29	1.57	0.19	0.27	0.20	0.09	0.25	2.00

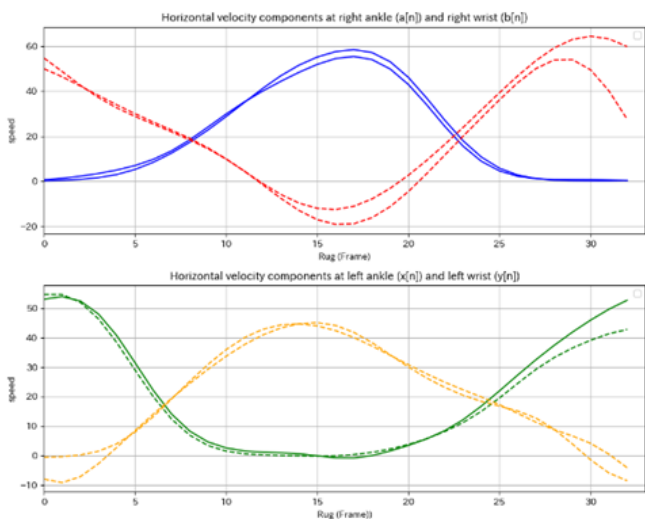


Fig. 7. Horizontal speed in motion S of subject 1. Blue: Right Ankle; Red: Right Wrist; Green: Left Ankle; Yellow: Left Wrist

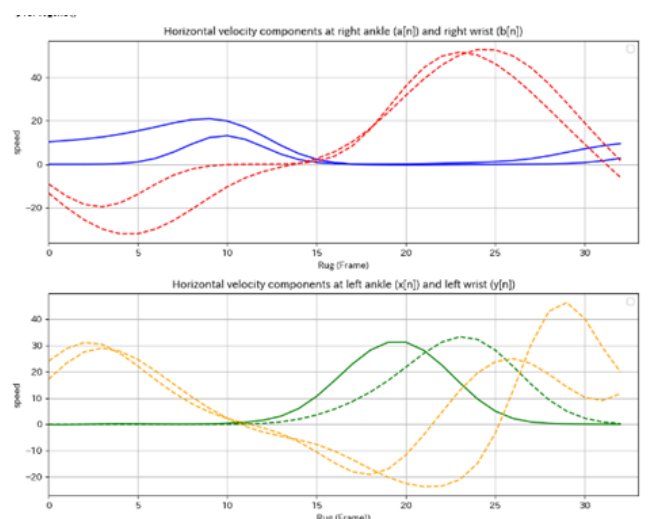


Fig. 9. Horizontal speed in motion A of subject 1. Blue: Right Ankle; Red: Right Wrist; Green: Left Ankle; Yellow: Left Wrist

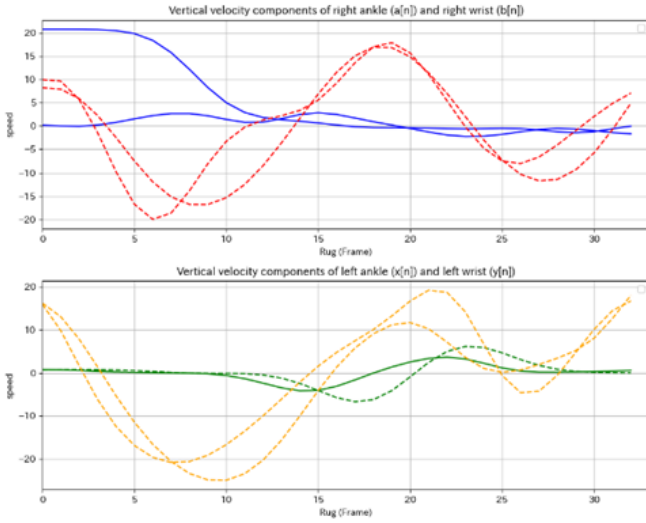


Fig. 10. Vertical speed in motion A of subject 1. Blue: Right Ankle; Red: Right Wrist; Green: Left Ankle; Yellow: Left Wrist

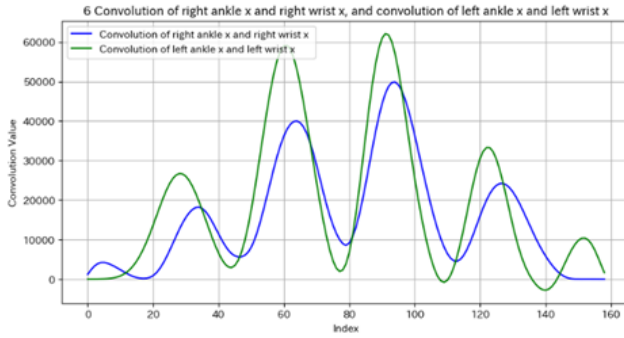


Fig. 11. Convolution computed case (HH) for motion S of subject 1

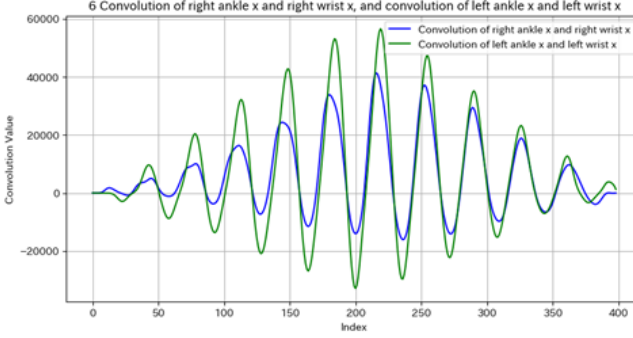


Fig. 12. Convolution computed case (HH) for motion A of subject 1

V. DISCUSSION

The effectiveness of the symmetry index, which shifts the motion by a total of half a cycle using a $\frac{1}{4}$ shift transformation for alternating periodic movements, was verified for the symmetric motion (S) and asymmetric motion (A) in five individuals.

When evaluating the dissimilarity of the transfer function from ankle movement to the movement of the ipsilateral wrist,

excluding case (HH), the asymmetric movement A showed a higher value, indicating greater asymmetry compared to the symmetric movement S. Clearly, asymmetric movements exhibited a high degree of dissimilarity in the left and right transfer functions. On the other hand, in asymmetric performances, all five participants showed similar left and right transfer functions for the horizontal movement of the ankle to the horizontal movement of the ipsilateral wrist in case (HH).

Figure 11 presents a box plot of the dissimilarity values for the five participants. The reason for the low dissimilarity in case (HHA) is that, while asymmetric movement A is a performance where intentional postures and movements can be expressed, the dynamic characteristics of the participants' motor coordination are instinctive, making it difficult to completely conceal their inherent left-right symmetry.

In this study, the input and output of the LTI system were represented as follows: $\vec{a}[n] \cdot \vec{e}_1$ and $\vec{b}[n] \cdot \vec{e}_1$, where the basis vectors \vec{e}_1 and \vec{e}_2 correspond to the horizontal and vertical directions, respectively. In the future, we aim to extend this approach by considering an LTI system that directly processes the two-dimensional vectors $\vec{a}[n]$ and $\vec{b}[n]$ as inputs and outputs.

In this extended framework, each convolution term $\vec{a}[n] \vec{y}[k - n]$ would not be a real number but rather the geometric product of vectors. Consequently, the dissimilarity measure would be defined as the ratio of the norms of complex numbers, ensuring a non-negative real value. A similar formulation can be derived for three-dimensional vectors, where the dissimilarity measure is defined as the ratio of the norms of quaternions.

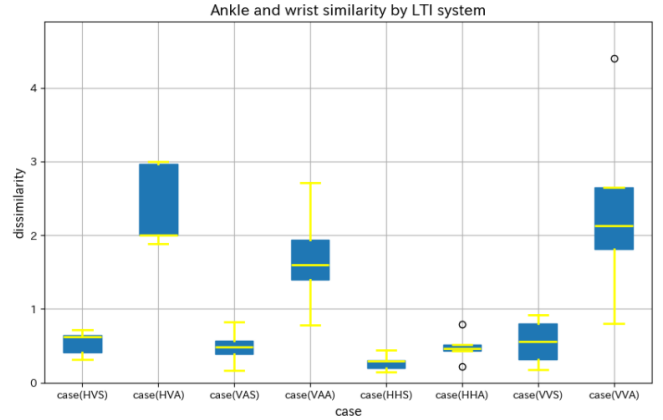


Fig. 13. Box-and-whisker diagram of dissimilarities evaluated for each case of 5 subjects

VI. CONCLUSION

In this study, we propose a dissimilarity measure for the left-side and right-side coupling systems underlying the time series pair (TSP) of two body points during walking, using video captured by a camera without the need for specialized equipment. We then examined whether the proposed measure can quantitatively assess left-right differences. When evaluating the left-right difference in transfer functions using an LTI

system, the transfer function from the horizontal movement of the ankle to the ipsilateral wrist in asymmetric movements showed similarity between the left and right sides, revealing the pedestrian's inherent left-right symmetry. All data and source code from this study are available at

REFERENCES

- [1] W. Wang, K. Li, N. Wei, C. Yin, and S. Yue, "Post-stroke asymmetry of muscle contractions for knee flexion and extension during walking," in *2016 9th International Congress on Image and Signal Processing, BioMedical Engineering and Informatics (CISP-BMEI)*, 2016, pp. 1712–1716.
- [2] ———, "Post-stroke asymmetry of muscle contractions for knee flexion and extension during walking," in *2016 9th International Congress on Image and Signal Processing, BioMedical Engineering and Informatics (CISP-BMEI)*, 2016, pp. 1712–1716.
- [3] R. Rathore, A. K. Singh, H. Chaudhary, and K. Kandan, "Gait abnormality detection in unilateral trans-tibial amputee in real-time gait using wearable setup," *IEEE Sensors Journal*, vol. 23, no. 12, pp. 12 567–12 573, 2023.
- [4] L. D'Arco, H. Wang, C. Wilson, E. Preatoni, E. Seminati, G. Trewartha, J. Cundell, and H. Zheng, "Smart insoles-based gait symmetry detection for people with lower-limb amputation," in *2024 35th Irish Signals and Systems Conference (ISSC)*, 2024, pp. 1–7.
- [5] I. Loiret, O. Rémy-Néris, P. Thoumie, N. Martinet, C. Detrembleur, W. De Neve, D. Slangen, E. Hanff, Y. Ruvalcaba, F. Molina-Rueda *et al.*, "Are wearable insoles a validated tool for quantifying transfemoral amputee gait asymmetry?" *Prosthetics and Orthotics International*, vol. 43, no. 5, pp. 492–499, 2019.
- [6] J. R. Williamson, A. Dumas, A. R. Hess, T. Patel, B. A. Telfer, and M. J. Buller, "Detecting and tracking gait asymmetries with wearable accelerometers," in *2015 IEEE 12th International Conference on Wearable and Implantable Body Sensor Networks (BSN)*, 2015, pp. 1–6.
- [7] S. Qin, B. Dai, J. Yan, P. Li, Z. Liu, and X. Chen, "Human gait symmetry analysis based on human electrostatic fields," *IEEE Sensors Journal*, vol. 23, no. 12, pp. 13 422–13 432, 2023.
- [8] X. Chen, J. Yan, S. Qin, P. Li, S. Ning, and Y. Liu, "Fall detection method based on a human electrostatic field and vmd-ecanet architecture," *IEEE Journal of Biomedical and Health Informatics*, vol. 29, no. 1, pp. 583–595, 2025.
- [9] S. Qin, D. Gao, X. Chen, S. Ning, Z. Liu, and P. Li, "Analysis of motor functions of hemiplegic patients based on dual-mode signal fusion," *IEEE Sensors Journal*, vol. 24, no. 20, pp. 32 694–32 706, 2024.
- [10] S. Qin, J. Yan, X. Chen, W. Li, P. Li, and Z. Liu, "Assessing the stability of human gait based on a human electrostatic field detection system," *IEEE Sensors Journal*, vol. 24, no. 7, pp. 11 036–11 047, 2024.
- [11] G. Yoge, M. Plotnik, C. Peretz, N. Giladi, and J. M. Hausdorff, "Gait asymmetry in patients with parkinson's disease and elderly fallers: when does the bilateral coordination of gait require attention?" *Experimental Brain Research*, vol. 177, no. 3, pp. 336–346, 2007.
- [12] P. G. Adamczyk and A. D. Kuo, "Mechanisms of gait asymmetry due to push-off deficiency in unilateral amputees," *IEEE Transactions on Neural Systems and Rehabilitation Engineering*, vol. 23, no. 5, pp. 776–785, 2015.
- [13] A. Sant'Anna and N. Wickström, "A symbol-based approach to gait analysis from acceleration signals: Identification and detection of gait events and a new measure of gait symmetry," *IEEE Transactions on Information Technology in Biomedicine*, vol. 14, no. 5, pp. 1180–1187, 2010.
- [14] W. Zhang, M. Smuck, C. Legault, M. A. Ith, A. Muaremi, and K. Aminian, "Gait symmetry assessment with a low back 3d accelerometer in post-stroke patients," *Sensors*, vol. 18, no. 10, p. 3322, 2018.
- [15] D. Gouwanda, "Further validation of normalized symmetry index and normalized cross-correlation in identifying gait asymmetry on restricted knee and ankle movement," in *2012 IEEE-EMBS Conference on Biomedical Engineering and Sciences*, 2012, pp. 423–427.
- [16] W. Sheng, W. Guo, F. Zha, Z. Jiang, X. Wang, and H. Zhang, "The effectiveness of gait event detection based on absolute shank angular velocity in turning," in *2019 IEEE 4th International Conference on Advanced Robotics and Mechatronics (ICARM)*, 2019, pp. 899–904.
- [17] A. C. Yep Khoo, Y. Ting Yap, D. Gouwanda, and A. A. Gopalai, "Examination of interlimb coordination of human asymmetric gait," in *2018 IEEE-EMBS Conference on Biomedical Engineering and Sciences (IECBES)*, 2018, pp. 680–685.
- [18] P. G. Arauz, A. H. Khandoker, W. C. Tay, V. Sundararajan, Y. H. Pua, K. C. Tan, J. H. Tan, and D. Gouwanda, "Spine and lower body symmetry during treadmill walking in healthy individuals—in-vivo 3-dimensional kinematic analysis," *PLOS ONE*, vol. 17, no. 10, p. e0275174, 2022.
- [19] H. L. Siebers, M. Mohr, and S. Grau, "Comparison of different symmetry indices for the quantification of dynamic joint angles," *BMC Sports Science, Medicine and Rehabilitation*, vol. 13, no. 1, p. 130, 2021.
- [20] C. Ochoa-Diaz and L. B. A. Padilha, "Symmetry analysis of amputee gait based on body center of mass trajectory and discrete fourier transform," *Sensors*, vol. 20, no. 8, p. 2392, 2020.